

Wave Motion 26 (1997) 1-12



Flexural wave propagation and scattering on thin plates using Mindlin theory

C. Vemula, A.N. Norris*

Department of Mechanical and Aerospace Engineering, Rutgers University, PO Box 909, Piscataway, NJ 08854-0909, USA

Received 24 June 1994; revised 4 December 1996

Abstract

The theory of scattering for flexural waves is developed for an elastic heterogeneity in a flat thin plate in the context of Mindlin's theory. Some new results are derived for energy flux and contrasted with the equivalent results in Kirchhoff plate theory. Numerical examples are presented for scattering of flexural waves from circular regions of inhomogeneity with different plate properties and are compared with similar results using the Kirchhoff plate theory.

1. Introduction

In an earlier paper [1] we studied the scattering of flexural waves from a heterogeneity in a flat thin plate in the context of Kirchhoff's thin plate theory. Here we derive some fundamental results for scattering of flexural waves using Mindlin's theory of transverse motion in thin plates [2,3]. The Mindlin theory is a better approximation of the underlying mechanics in a thin plate but introduces analytical complications as compared with the simpler formulation. Mindlin's theory contains two rotations as field variables in addition to the transverse displacement and includes rotary inertia and shear effects which are ignored in the Kirchhoff theory.

The problem of diffractions of flexural waves by a circular cavity in an elastic plate has been solved by Pao and Chao [4] and by a rigid circular inclusion by Lu [5]. Both papers [4,5] were concerned primarily with the dynamic moment and stress concentration factors, and provided detailed calculations of these based on Mindlin theory. In this paper we develop the ideas of energy flux conservation and derive an optical theorem for flexural waves. Similar results were presented earlier in [1] in the context of Kirchhoff theory. Backscattered far-field amplitudes are numerically computed for scattering of flexural waves from a circular heterogeneity with different plate properties. The problems solved by Pao and Chao and Lu are special cases of this formulation.

^{*} Corresponding author. E-mail: norris@norris.rutgers.edu.

2. Displacement potentials for Mindlin plate theory

Mindlin's approximate theory for flexural waves in plates is well known and can be found in many textbooks, for example [6]. The theory includes shear-deformation and rotary-inertia effects, as in the Timoshenko beam theory. The equations of motion restrict the deformation to three degrees of freedom, and they are obtained by averaging the exact equations of elasticity across the plate thickness. The deformation at any point is given by the three-dimensional displacement defined by the kinematic relation

$$\mathbf{u} = z \nabla \cdot \psi(\mathbf{x}, t) + w(\mathbf{x}, t) \mathbf{e}_z, \tag{1}$$

where \mathbf{x} is the two-dimensional position vector defining a point on the central plane of the plate, and z is the coordinate transverse to this plane. Note that the transverse displacement w is independent of z, so that thickness modes (stretch and shear) are ignored in this approximation. Also, $\psi \perp \mathbf{e}_z$ denotes the two-dimensional vector of rotations.

For a given direction \mathbf{n} , $|\mathbf{n}| = 1$, with s designating the direction perpendicular to \mathbf{n} , the bending and twisting moments and the shear forces are

$$M_n = D\left\{\frac{\partial \psi_n}{\partial n} + \nu \frac{\partial \psi_s}{\partial s}\right\},\tag{2a}$$

$$M_s = D \left\{ \frac{\partial \psi_s}{\partial s} + \nu \frac{\partial \psi_n}{\partial n} \right\},\tag{2b}$$

$$M_{ns} = \frac{1}{2}D(1-\nu)\left\{\frac{\partial\psi_s}{\partial n} + \frac{\partial\psi_n}{\partial s}\right\},\tag{2c}$$

$$Q_n = \overline{\mu} \left\{ \frac{\partial w}{\partial n} + \psi_n \right\},\tag{2d}$$

$$Q_s = \overline{\mu} \left\{ \frac{\partial w}{\partial s} + \psi_s \right\},\tag{2e}$$

where $D = Eh^3/12(1-v^2)$, $\overline{\mu} = \alpha^2 h\mu$, and E, μ, α^2, v and h are Young's modulus, the shear modulus, a shear coefficient, Poisson's ratio and the thickness, respectively. A weighted average of τ_{zz} is neglected in deriving the above relations. As a consequence of both this and the kinematical assumptions, a modified shear modulus, $\overline{\mu}$, is used in order to obtain the exact shear forces. Normally, $\alpha^2 \le 1$ [6].

The plate equations of motion are:

$$\frac{\partial M_n}{\partial n} + \frac{\partial M_{ns}}{\partial s} - Q_n = \frac{mh^2}{12} \frac{\partial^2 \psi_n}{\partial t^2},\tag{3a}$$

$$\frac{\partial M_{ns}}{\partial n} + \frac{\partial M_s}{\partial s} - Q_s = \frac{mh^2}{12} \frac{\partial^2 \psi_s}{\partial t^2},\tag{3b}$$

$$\frac{\partial Q_n}{\partial r} + \frac{\partial Q_s}{\partial s} + q = m \frac{\partial^2 w}{\partial t^2},\tag{3c}$$

where $m = \rho h$ is the mass density per unit area, and q the external loading on the plate. When the plate stress-displacement equations (2) are substituted in the preceding equations, we obtain

$$\frac{D}{2}\{(1-\nu)\nabla^2\psi + (1+\nu)\nabla\nabla\cdot\psi\} - \overline{\mu}(\psi + \nabla w) = \frac{mh^2}{12}\frac{\partial^2\psi}{\partial t^2},\tag{4a}$$

$$\overline{\mu}(\nabla^2 w + \nabla \cdot \psi) + q = m \frac{\partial^2 w}{\partial t^2}.$$
 (4b)

The general solution for time harmonic motion in the absence of an applied load can be written in the form $w(\mathbf{x}, t) = \text{Re}[W(\mathbf{x})e^{-i\omega t}]$ and $\psi(\mathbf{x}, t) = \text{Re}[\Psi(\mathbf{x})e^{-i\omega t}]$ where

$$\boldsymbol{W} = W_1 + W_2, \qquad \boldsymbol{\Psi} = A_1 \nabla W_1 + A_2 \nabla W_2 - \mathbf{e}_z \times \nabla V, \tag{5}$$

and W_1 , W_2 and V each satisfy Helmholtz equations,

$$\nabla^2 W_1 + k_1^2 W_1 = 0, (6a)$$

$$\nabla^2 W_2 + k_2^2 W_2 = 0, (6b)$$

$$\nabla^2 V + k_3^2 V = 0. ag{6c}$$

These solutions are analogous to dilatational and equivoluminal potentials in three-dimensional elasticity [7]. The wave numbers k_1 , k_2 and k_3 are determined by

$$k_{1,2}^2 = \frac{1}{2}(k_{\rm p}^2 + k_{\rm s}^2) \pm \sqrt{k_{\rm f}^4 + \frac{1}{4}(k_{\rm p}^2 - k_{\rm s}^2)^2},\tag{7a}$$

$$k_3^2 = \alpha^2 \frac{k_1^2 k_2^2}{k_p^2},\tag{7b}$$

where

$$k_{\rm s} = \frac{\omega}{c_{\rm s}}, \qquad k_{\rm p} = \frac{\omega}{c_{\rm p}}, \qquad k_f = \left(\frac{m\omega^2}{D}\right)^{1/4}, \quad c_{\rm s} = \left(\frac{\overline{\mu}}{m}\right)^{1/2}, \quad c_{\rm p} = \left[\frac{E}{\rho(1-v^2)}\right]^{1/2}.$$
 (8)

Also.

$$A_j = -1 + \frac{k_s^2}{k_j^2}, \quad j = 1, 2.$$
 (9)

The general solution of Eq. (5), first obtained by Mindlin [2], is derived in Appendix A by a slightly different approach.

We note that $k_{\rm f}$ is the wave number of flexural waves in the Kirchhoff theory. By their definitions, $k_{\rm l}^2 > 0$ always and $k_{\rm l}^2 < 0$ for $\omega < \sqrt{12}c_{\rm s}/h$. We also note that $k_{\rm l}^2 < 0$ whenever $k_{\rm l}^2 < 0$, and that at the cutoff frequency $\sqrt{12}c_{\rm s}/h$ the "bulk" shear wave number $k_{\rm s}$ is of the same order as 1/h, putting the validity of the theory into question for frequencies at or above cutoff. Therefore, for all practical purposes $k_{\rm l}$ and $k_{\rm l}$ are purely imaginary, corresponding to evanescent types of wave motion.

3. Energy flux conservation

3.1. Definition of the energy flux

We now derive some general expressions related to energy flux for bending waves. The pointwise expression of conservation of mechanical energy, in the absence of an external source, can be written

$$\frac{\partial U}{\partial t} + \nabla \cdot \mathbf{F} = 0,\tag{10}$$

where U is the full energy density (per unit area) and \mathbf{F} is the energy flux vector. The component of the energy flux vector in the \mathbf{n} -direction is [6]:

$$F_n = -\left(Q_n \frac{\partial w}{\partial t} + M_n \frac{\partial \psi_n}{\partial t} + M_{ns} \frac{\partial \psi_s}{\partial t}\right),\tag{11}$$

or, using the previous definitions,

$$F_n = -\overline{\mu} \left(\frac{\partial w}{\partial n} + \psi_n \right) \frac{\partial w}{\partial t} - D \left[\frac{\partial \psi_n}{\partial n} + \nu \frac{\partial \psi_s}{\partial s} \right] \frac{\partial \psi_n}{\partial t} - \frac{1}{2} D (1 - \nu) \left[\frac{\partial \psi_n}{\partial s} + \frac{\partial \psi_s}{\partial n} \right] \frac{\partial \psi_s}{\partial t}. \tag{12}$$

Expression (11) for the bending power flow directly follows from the general definition of the power flow in linear elasticity theory [8]. Applying the conservation relation (10) to a simply connected area A with boundary C and outward normal \mathbf{n} , gives

$$\frac{\partial}{\partial t} \int_{A} U \, \mathrm{d}A + \int_{C} F_n \, \mathrm{d}s = 0. \tag{13}$$

The boundary integral can be simplified by rewriting Eq. (12) as

$$F_n = \widehat{F}_n + D(1 - \nu) \left[\frac{\partial \psi_s}{\partial s} \frac{\partial \psi_n}{\partial t} - \frac{\partial \psi_n}{\partial s} \frac{\partial \psi_s}{\partial t} \right], \tag{14}$$

where

$$\widehat{F}_n \equiv -\overline{\mu} \left(\frac{\partial w}{\partial n} + \psi_n \right) \frac{\partial w}{\partial t} - D \left[(\nabla \cdot \psi) \frac{\partial \psi_n}{\partial t} + \frac{1}{2} (1 - \nu) \mathbf{e}_z \cdot (\nabla \times \psi) \frac{\partial \psi_s}{\partial t} \right]. \tag{15}$$

Integrating by parts with respect to s, Eq. (13) reduces to

$$\frac{\partial}{\partial t} \left\{ \int_{A} U \, dA + D(1 - \nu) \int_{C} \psi_{n} \frac{\partial \psi_{s}}{\partial s} \, ds \right\} + \int_{C} \widehat{F}_{n} \, ds = 0.$$
 (16)

We now assume the motion is periodic and define the time average of a physical quantity f over one period as $\langle f \rangle$. Averaging the energy conservation relation (13) implies that the surface integral of the flux $\langle F_n \rangle$ vanishes for any contour not enclosing sources. However, according to Eq. (16), the same is true of the "simplified" flux $\langle \widehat{F}_n \rangle$. Thus, although $\widehat{\mathbf{F}}$ is not the instantaneous flux, its time average coincides with the time average of the true flux. The simpler form of $\widehat{\mathbf{F}}$ makes it more suitable for using in practice to check the conservation of energy. To be specific, we consider time harmonic motion for which the energy conservation relation is

$$0 = \int_{C} \langle F_{n} \rangle \, \mathrm{d}s = \int_{C} \langle \widehat{F}_{n} \rangle \, \mathrm{d}s$$

$$= \frac{\omega}{2} \mathrm{Im} \int_{C} \left\{ -\overline{\mu} W \left(\frac{\partial W^{*}}{\partial n} + \Psi_{n}^{*} \right) - D \left[\Psi_{n} \nabla \cdot \boldsymbol{\varPsi}^{*} + \frac{1}{2} (1 - \nu) \Psi_{s} \left(\mathbf{e}_{z} \cdot \nabla \times \boldsymbol{\varPsi}^{*} \right) \right] \right\} \, \mathrm{d}s, \tag{17}$$

where we have used the definition of \widehat{F}_n in Eq. (15) and * denotes the complex conjugate.

It is interesting to contrast this result with its equivalent in Kirchhoff's theory, which is [1,9]:

$$\omega \frac{D}{2} \operatorname{Im} \int_{C} \left(W \frac{\partial}{\partial n} \nabla^{2} W^{*} - \nabla^{2} W^{*} \frac{\partial W}{\partial n} \right) ds = 0.$$
 (18)

In comparing Eqs. (17) and (18) we first note that the term $\overline{\mu} \left(\partial W^* / \partial n + \Psi_n^* \right)$ is Q_n^* , according to Eq. (2d). However, Q_n^* is $-D\partial \nabla^2 W^* / \partial n$ in Kirchhoff plate theory, and therefore the first term in the brackets in Eq. (18) can be identified with first term in the curly brackets in Eq. (17). The term $\Psi_n \nabla \cdot \Psi^*$ is $(\partial W / \partial n) \nabla^2 W^*$ in the Kirchhoff plate theory. Thus, the second term in the brackets in Eq. (18) is equivalent to the first term in square brackets in

Eq. (17). Finally, the term $\nabla \times \Psi^*$ is zero in the Kirchhoff theory. Thus, there is no term in the Kirchhoff result, Eq. (18), which is equivalent to the second term in square brackets in Eq. (17).

Finally, we note that Eq. (17) may be simplified in terms of the potentials of the previous section. The general solutions (5) produce the identity

$$\operatorname{Im} \int_{C} \left\{ \overline{\mu} W \left(\frac{\partial W^*}{\partial n} + \Psi_n^* \right) + D \left[-\Psi_n (A_1 k_1^2 W_1^* + A_2 k_2^2 W_2^*) + \frac{(1 - \nu)}{2} \Psi_s k_3^2 V^* \right] \right\} ds = 0.$$
 (19)

3.2. An optical theorem for flexural waves

Consider a finite region of an otherwise homogeneous plate of infinite extent which contains a *scatterer*, which is by definition some type of obstacle that causes scattering of incident waves. It may consist of a region with different plate properties (thickness, density, etc.) or it could be an attachment of some type. The solution of Eqs. (5), for W and Ψ , simplify in the far field to

$$\boldsymbol{W} = \boldsymbol{W}_1, \qquad \boldsymbol{\Psi} = \boldsymbol{A}_1 \nabla \boldsymbol{W}_1, \tag{20}$$

because, k_2 and k_3 are real only for very high frequencies and hence the corresponding waves do not propagate to the far field for frequencies of interest. The flux identity (19) also simplifies in the far field, to give

$$\operatorname{Im} \int_{C} \left\{ \overline{\mu} \left[1 + A_1 \right] W_1 \frac{\partial W_1^*}{\partial n} - D A_1^2 k_1^2 W_1^* \frac{\partial W_1}{\partial n} \right\} ds = 0.$$
 (21)

The identity (21) applies to the flux generated by the *total* field, but not to the flux defined by the scattered part of the response, $W_1^{\rm sc} = W_1 - W_1^{\rm inc}$. Here $W_1^{\rm inc}$ is the incident wave, which we assume to be a straight-crested wave. Define the scattered far-field amplitude $f(\theta)$ such that

$$W_1^{\text{sc}} = \frac{1}{\sqrt{2r}} e^{i(k_1 r - \pi/4)} f(\theta) + o(1/\sqrt{r}), \quad r \to \infty.$$
 (22)

The scattered flexural displacement can always be expanded in a set of complete wave functions. Thus, the general form of the scattered far field can be represented as [10]:

$$W_1^{\text{sc}} = \sum_{n=0}^{\infty} H_n^{(1)}(k_1 r) (B_n \cos n\theta + B_n' \sin n\theta), \tag{23}$$

where $B_0' = 0$. This type of representation is appropriate for scatterers of circular shape, and will be used in Section 4. Eq. (23) may also be used for arbitrary scattering configurations, although other basis functions might be appropriate if the geometry is separable, such as for elliptical regions [10]. The far-field amplitude follows from the definition in (22) and the asymptotic behavior of Hankel functions,

$$f(\theta) = \frac{2}{\sqrt{\pi k_1}} \sum_{n=0}^{\infty} (-i)^n (B_n \cos n\theta + B'_n \sin n\theta). \tag{24}$$

The average energy flux of the incident wave $W_1^{\text{inc}} = e^{ik_1x} = e^{ik_1r\cos\theta}$ across a unit length of any wavefront, x = constant, follows from Eqs. (12) and (20) as

$$\langle F^{\rm inc} \rangle = \frac{1}{2} \omega [Dk_1^3 A_1^2 + \overline{\mu} k_1 (1 + A_1)].$$
 (25)

The energy flux associated with the scattered field follows by substituting (22) into the left-hand side of (21) and multiplying with $\frac{1}{2}\omega$ while letting the contour C recede to infinity. The scattering cross-section, σ^{sc} , defined as the ratio of the latter flux to the incident flux, is therefore

$$\sigma^{\text{sc}} = \frac{1}{2} \int_{0}^{2\pi} |f(\theta)|^2 \, \mathrm{d}\theta. \tag{26}$$

Note that σ^{sc} has dimensions of length. Assuming that the scatterer does not dissipate energy, we may apply the energy flux result (21). Thus, replace the total field in (21) using the incident wave and the far-field scattered response, and again let the contour tend to infinity. The flux across C associated with the incident wave vanishes, while the remaining terms give

$$\int_{0}^{2\pi} |f(\theta)|^2 d\theta + \lim_{r \to \infty} \sqrt{2r} \operatorname{Re} \left\{ e^{-i\pi/4} \int_{0}^{2\pi} (1 + \cos \theta) e^{ik_1 r (1 - \cos \theta)} f(\theta) d\theta \right\} = 0.$$
 (27)

The limit can be evaluated by first approximating the integral asymptotically using the method of stationary phase and then taking the limit, to yield, using (26),

$$\sigma^{\rm sc} = -2\sqrt{\frac{\pi}{k}} \operatorname{Re} f(0). \tag{28}$$

The optical theorem of classical acoustics and electromagnetics [11] is an expression of energy conservation, and Eq. (28) is the analog for the Mindlin theory. An identical optical theorem applies to the Kirchhoff plate theory, as discussed in [1]. Although the flux appears to be quite different in form in both theories, the fact that the far-field flexural waves are governed by Helmholtz equations makes the form of the optical theorem identical to that of two-dimensional acoustics for either plate theory. Finally, we note that Eqs. (24), (26) and the optical theorem (28) imply the identity

$$|B_0|^2 + \operatorname{Re} B_0 + \sum_{n=1}^{\infty} \left\{ \frac{|B_n|^2}{2} + \frac{|B_n'|^2}{2} + \operatorname{Re}[(-i)^n B_n] \right\} = 0.$$
 (29)

This serves as a numerical check on any computed results, and was used in the examples discussed next.

4. Scattering by a cylindrical inhomogeneity

4.1. General solution

We consider a circular region of inhomogeneity in $r \le a$, which is perfectly bonded to the exterior region along the boundary r = a. Let the exterior, infinite plate be denoted by 1, and the scatterer by 2, so that the properties in each region are D_j , v_j , ρ_j and h_j , j = 1, 2. Time harmonic motion is assumed, so the wave numbers are k_{11} , k_{21} , k_{31} , k_{12} , k_{22} and k_{32} , where the second suffix refers to the region. The incident wave is of the first type, flexural, and propagating in the positive x-direction.

The cylindrical coordinate solutions for the displacements W_j , j = 1, 2, in Eq. (6), are the Bessel functions $H_n^{(1)}(k_jr)$ and $J_n(k_jr)$, while the solutions for V in Eq. (7b) are $H_n^{(1)}(k_3r)$ and $J_n(k_3r)$. Thus, the total displacement is of the form

$$W = \begin{cases} e^{ik_{11}r\cos\theta} + \sum_{n=0}^{\infty} [B_{1n}H_n^{(1)}(k_{11}r) + B_{2n}H_n^{(1)}(k_{21}r)]\cos n\theta, & r > a, \\ \sum_{n=0}^{\infty} [B_{4n}J_n(k_{12}r) + B_{5n}J_n(k_{22}r)]\cos n\theta, & r \le a, \end{cases}$$
(30)

$$\psi_{r} = \begin{cases} A_{11} \frac{\partial}{\partial r} e^{ik_{11}r\cos\theta} + \sum_{n=0}^{\infty} [A_{11}B_{1n}k_{11}H_{n}^{(1)'}(k_{11}r) + A_{21}B_{2n}k_{21}H_{n}^{(1)'}(k_{21}r) \\ + (B_{3n}n/r)H_{n}^{(1)}(k_{31}r)]\cos n\theta, \quad r > a, \\ \sum_{n=0}^{\infty} [A_{12}B_{4n}k_{12}J_{n}^{'}(k_{12}r) + A_{22}B_{5n}k_{22}J_{n}^{'}(k_{22}r) + (B_{6n}n/r)J_{n}(k_{32}r)]\cos n\theta, \quad r \leq a, \end{cases}$$
(31)

$$W = \begin{cases} e^{ik_{11}r\cos\theta} + \sum_{n=0}^{\infty} [B_{1n}H_n^{(1)}(k_{11}r) + B_{2n}H_n^{(1)}(k_{21}r)]\cos n\theta, & r > a, \\ \sum_{n=0}^{\infty} [B_{4n}J_n(k_{12}r) + B_{5n}J_n(k_{22}r)]\cos n\theta, & r \leq a, \end{cases}$$

$$\psi_r = \begin{cases} A_{11}\frac{\partial}{\partial r}e^{ik_{11}r\cos\theta} + \sum_{n=0}^{\infty} [A_{11}B_{1n}k_{11}H_n^{(1)'}(k_{11}r) + A_{21}B_{2n}k_{21}H_n^{(1)'}(k_{21}r) \\ + (B_{3n}n/r)H_n^{(1)}(k_{31}r)]\cos n\theta, & r > a, \end{cases}$$

$$\sum_{n=0}^{\infty} [A_{12}B_{4n}k_{12}J_n'(k_{12}r) + A_{22}B_{5n}k_{22}J_n'(k_{22}r) + (B_{6n}n/r)J_n(k_{32}r)]\cos n\theta, & r \leq a, \end{cases}$$

$$\psi_\theta = \begin{cases} -(A_{11}/r)\frac{\partial}{\partial \theta}e^{ik_{11}r\cos\theta} - \sum_{n=0}^{\infty} [(A_{11}B_{1n}n/r)H_n^{(1)}(k_{11}r) + (A_{21}B_{2n}n/r)H_n^{(1)}(k_{21}r) \\ + B_{3n}k_{31}H_n^{(1)'}(k_{31}r)]\sin n\theta, & r > a, \\ -\sum_{n=0}^{\infty} [(A_{12}B_{4n}n/r)J_n(k_{12}r) + (A_{22}B_{5n}n/r)J_n(k_{22}r) + B_{6n}k_{32}J_n'(k_{32}r)]\sin n\theta, & r \leq a, \end{cases}$$
(32)
$$\text{Te } B_{1n}, B_{2n}, B_{3n}, B_{4n}, B_{5n}, B_{6n}, n = 0, 1, \dots, \text{ are constants, and again the second suffix on } A_{ii}, i = 1, 2, \text{ refers} \end{cases}$$

where B_{1n} , B_{2n} , B_{3n} , B_{4n} , B_{5n} , B_{6n} , $n = 0, 1, \ldots$, are constants, and again the second suffix on A_{ij} , j = 1, 2 refers to the region. The choice of the wave functions is dictated by the conditions that the scattered response is finite at r=0 and must be outgoing, or radiating, as $r\to\infty$. There are six continuity conditions on r=a, requiring that W, $\psi_r, \psi_\theta, M_r, M_{r\theta}$, and Q_r are continuous across the boundary. We note that $e^{ik_{11}r\cos\theta} = \sum_{n=0}^{\infty} \epsilon_n i^n J_n(k_{11}r)\cos n\theta$, where $\epsilon_0 = 1$, $\epsilon_n = 2$, $n \ge 1$, and also that the quantities defined in Eqs. (2a), (2c), and (2d), become in cylindrical coordinates.

$$M_r = D\left[\frac{\partial \psi_r}{\partial r} + \frac{v}{r}\left(\frac{\partial \psi_\theta}{\partial \theta} + \psi_r\right)\right] = D\left[\nabla \cdot \psi - \frac{(1-v)}{r}\left(\psi_r + \frac{\partial \psi_\theta}{\partial \theta}\right)\right],\tag{33a}$$

$$M_{r\theta} = \frac{D}{2}(1 - \nu) \left[\frac{\partial \psi_{\theta}}{\partial r} + \frac{1}{r} \frac{\partial \psi_{r}}{\partial \theta} - \frac{\psi_{\theta}}{r} \right] = \frac{D}{2}(1 - \nu) \left[\mathbf{e}_{z} \cdot \nabla \times \psi - \frac{2}{r} \left(\psi_{\theta} - \frac{\partial \psi_{r}}{\partial \theta} \right) \right], \tag{33b}$$

$$Q_r = \overline{\mu} \left(\frac{\partial w}{\partial r} + \psi_r \right). \tag{33c}$$

Applying the continuity conditions for each azimuthal order n = 0, 1, 2, ..., we arrive at the following set of equations for the unknowns.

tions for the unknowns.

$$\begin{bmatrix} H_n^{(1)}(\kappa_{11}) & H_n^{(1)}(\kappa_{21}) & 0 & J_n(\kappa_{12}) & J_n(\kappa_{22}) & 0 \\ S_{1H}(\kappa_{11}) & S_{1H}(\kappa_{21}) & T_{1H}(\kappa_{31}) & S_{1J}(\kappa_{12}) & S_{1J}(\kappa_{22}) & T_{1J}(\kappa_{32}) \\ S_{2H}(\kappa_{11}) & S_{2H}(\kappa_{21}) & T_{2H}(\kappa_{31}) & S_{2J}(\kappa_{12}) & S_{2J}(\kappa_{22}) & T_{2J}(\kappa_{32}) \\ S_{3H}(\kappa_{11}) & S_{3H}(\kappa_{21}) & T_{3H}(\kappa_{31}) & S_{3J}(\kappa_{12}) & S_{3J}(\kappa_{22}) & T_{3J}(\kappa_{32}) \\ S_{4H}(\kappa_{11}) & S_{4H}(\kappa_{21}) & T_{4H}(\kappa_{31}) & S_{4J}(\kappa_{12}) & S_{4J}(\kappa_{22}) & T_{4J}(\kappa_{32}) \\ S_{5H}(\kappa_{11}) & S_{5H}(\kappa_{21}) & T_{5H}(\kappa_{31}) & S_{5J}(\kappa_{12}) & S_{5J}(\kappa_{22}) & T_{5J}(\kappa_{32}) \end{bmatrix} \begin{pmatrix} -B_{1n} \\ -B_{2n} \\ -B_{3n} \\ B_{4n} \\ B_{5n} \\ B_{6n} \end{pmatrix} = \epsilon_n i^n \begin{cases} J_n(\kappa_{11}) \\ S_{1J}(\kappa_{11}) \\ S_{3J}(\kappa_{11}) \\ S_{4J}(\kappa_{11}) \\ S_{5J}(\kappa_{11}) \end{cases}.$$
(34)

The following notation is used for each n:

$$S_{1X}(\kappa_{ij}) = A_{ij}\kappa_{ij}X_n'(\kappa_{ij}), \tag{35a}$$

$$S_{2X}(\kappa_{ij}) = A_{ij} n X_n(\kappa_{ij}), \tag{35b}$$

$$S_{3X}(\kappa_{ij}) = D_j A_{ij} [\kappa_{ij}^2 X_n(\kappa_{ij}) + (1 - \nu_j) \kappa_{ij} X_n'(\kappa_{ij}) - (1 - \nu_j) n^2 X_n(\kappa_{ij})],$$
(35c)

$$S_{4X}(\kappa_{ij}) = D_j A_{ij} (1 - \nu_j) n[X_n(\kappa_{ij}) - \kappa_{ij} X_n'(\kappa_{ij})], \tag{35d}$$

$$S_{5X}(\kappa_{ij}) = \overline{\mu}_{j}\kappa_{ij}(1 + A_{ij})X_{n}^{'}(\kappa_{ij})$$
(35e)

$$T_{1X}(\kappa_{ij}) = na^2 X_n(\kappa_{ij}), \tag{35f}$$

$$T_{2X}(\kappa_{ij}) = a^2 \kappa_{ij} X_n'(\kappa_{ij}), \tag{35g}$$

$$T_{3X}(\kappa_{ij}) = D_j na^2 (1 - \nu_j) [X_n(\kappa_{ij}) - \kappa_{ij} X'_n(\kappa_{ij})], \tag{35h}$$

$$T_{4X}(\kappa_{ij}) = D_j a^2 (1 - \nu_j) [(1/2)\kappa_{ij}^2 X_n(\kappa_{ij}) + \kappa_{ij} X_n'(\kappa_{ij}) - n^2 X_n(\kappa_{ij})], \tag{35i}$$

$$T_{5X}(\kappa_{ij}) = \overline{\mu}_j n a^2 X_n(\kappa_{ij}), \tag{35j}$$

for $X = H^{(1)}$, J; i = 1, 2, 3, and j = 1, 2, where $\kappa_{ij} = k_{ij}a$. The Helmholtz relations for W and V are used in simplifying the continuity conditions for M_r and $M_{r\theta}$.

4.2. Rigid and soft limits

There are two limits of interest corresponding to the cases in which the heterogeneity is either rigid or soft. The former corresponds to clamped conditions at r=a, while the soft limit gives a hole in r < a. In either case, only the field for $r \ge a$ is meaningful in Eqs. (30)–(32), and the matrix system (34) reduces to a 3×3 system. For the rigid limit, the matrix comes from the upper left block in (34), and gives (dropping the subscript 1 as redundant)

$$\begin{cases}
B_{1n} \\
B_{2n} \\
B_{3n}
\end{cases} = -\epsilon_n i^n \begin{bmatrix}
H_n^{(1)}(\kappa_1) & H_n^{(1)}(\kappa_2) & 0 \\
S_{1H}(\kappa_1) & S_{1H}(\kappa_2) & T_{1H}(\kappa_3) \\
S_{2H}(\kappa_1) & S_{2H}(\kappa_2) & T_{2H}(\kappa_3)
\end{bmatrix}^{-1} \begin{bmatrix}
J_n(\kappa_1) \\
S_{1J}(\kappa_1) \\
S_{2J}(\kappa_1)
\end{bmatrix}.$$
(36)

The matrix system for the case of a circular hole corresponds to the lower left block in (34), and yields

$$\begin{cases}
B_{1n} \\
B_{2n} \\
B_{3n}
\end{cases} = -\epsilon_n i^n \begin{bmatrix} S_{3H}(\kappa_1) & S_{3H}(\kappa_2) & T_{3H}(\kappa_3) \\
S_{4H}(\kappa_1) & S_{4H}(\kappa_2) & T_{4H}(\kappa_3) \\
S_{5H}(\kappa_1) & S_{5H}(\kappa_2) & T_{5H}(\kappa_3) \end{bmatrix}^{-1} \begin{cases}
S_{3J}(\kappa_1) \\
S_{4J}(\kappa_1) \\
S_{5J}(\kappa_1)
\end{cases} .$$
(37)

5. Numerical examples and conclusion

We illustrate the scattering theory for a steel plate of thickness $h_1 = 0.0254$ m. The dispersion curves for the three wave types are shown in Fig. 1 for real values of the wave number. The waves associated with k_2 and k_3 possess imaginary wave numbers for f < 63.8 kHz for this example. The "polarization" parameters A_1 and A_2

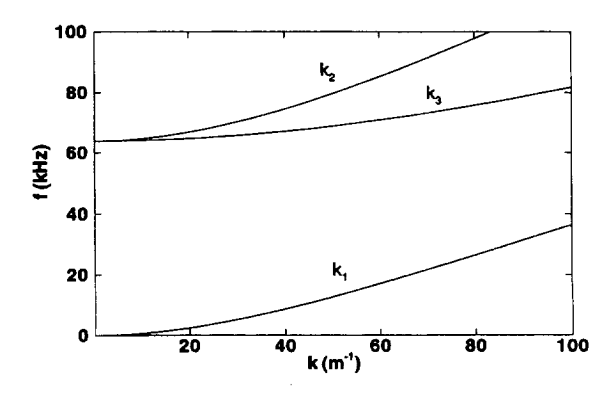


Fig. 1. Dispersion curves for a steel plate of 0.0254 m thickness.

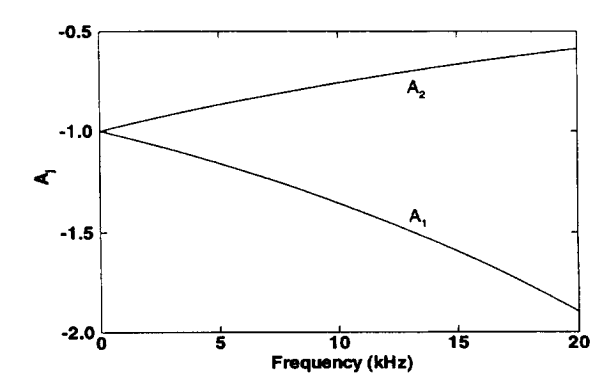


Fig. 2. The dimensionless parameters A_1 and A_2 . The plate is steel of 0.0254 m thickness.

associated with the wave modes with non-zero deflection are shown in Fig. 2. Note that both approximate -1 at low frequencies, in agreement with the expected value of the classical Kirchhoff theory.

Figs. 3-5 display far-field scattering data for an incident flexural wave on the same plate with different types of circular inclusions. A steel inclusion of thickness 1/25th of the plate thickness and radius $a=5h_1$ is considered in Fig. 3. The extremely thin nature of the inclusion makes it act, to a first approximation, like a hole of the same size. The response for such a hole is shown for comparison. Note that the inclusion approximates the hole response except at narrow frequency bands, which coincide with the resonant frequencies for free oscillation of the inclusion in the absence of the exterior plate. These are the modes with clamped boundary conditions on the circular rim of the inner thin plate. The backscatter from a rigid inclusion of the same radius is also given in Fig. 3. Note the singular nature of the backscatter as the frequency tends to zero, the static limit. This is to be expected, and has been discussed in a previous paper for the Kirchhoff plate theory [1].

A comparison of the predicted backscatter from circular rigid and soft (hole) inclusions is shown in Fig. 4. Note the response from the rigid inclusion is almost identical for both the Mindlin and Kirchhoff plate theories, but the hole has a more pronounced effect upon the backscatter in the Mindlin theory. This difference is significant even at frequencies far below the critical cut-on frequency for modes 2 and 3 (63.8 kHz), which is at $k_{11}a = 19.7$. Finally, Fig. 5 shows the different scattering predictions of the two theories for an inclusion of the same radius but of twice the thickness of the surrounding plate. Again, there is a sizeable difference even at relatively low frequencies. We expect that the Mindlin theory is more faithful to the physics of the problem as it contains more degrees of freedom

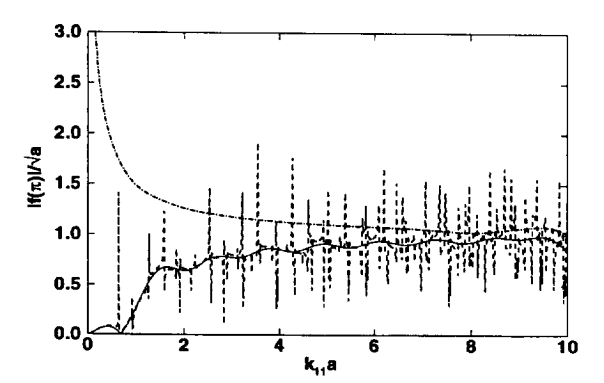


Fig. 3. The magnitude of the backscattered far-field flexural response for an incident wave of unit amplitude. The surrounding plate is steel of thickness h_1 and the inhomogeneity is of radius $a = 5h_1$. The three curves shown are: (——) the limiting case of a hole; (-----) a rigid inclusion; and (----) an inclusion of the same material but of thickness $h_1/25$.

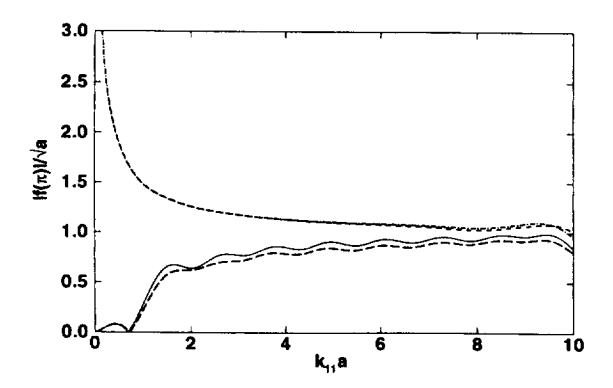


Fig. 4. Comparison of the magnitude of the backscattered far-field flexural response for an incident wave of unit amplitude, obtained using the Mindlin theory and the Kirchhoff theory. The surrounding plate is steel of thickness h_1 . The inhomogeneity is of radius $a = 5 h_1$ and thickness h_1 . The four curves shown are: (——) the limiting case of a hole in the Mindlin theory; (----) a rigid inclusion in the Mindlin theory; (----) the limiting case of a hole in the Kirchhoff theory; and (------) a rigid inclusion in Kirchhoff theory.

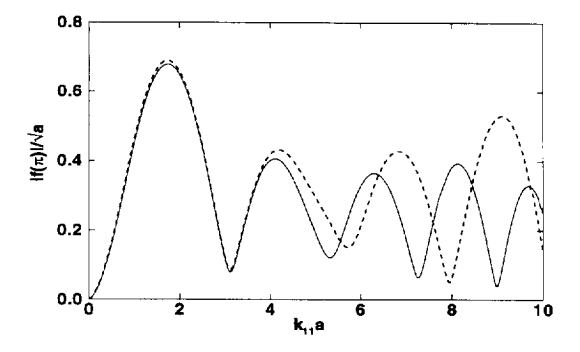


Fig. 5. Comparison of the magnitude of the backscattered far-field flexural response for an incident wave of unit amplitude, obtained using the Mindlin theory and the Kirchhoff theory. The surrounding plate is steel of thickness h_1 . The inhomogeneity is of radius $a = 5h_1$ and thickness $h_2 = 2h_1$. The two curves shown are: (——) Mindlin theory; (- - - -) Kirchhoff theory.

which in turn provide a better approximation of the actual interface conditions between the inclusion and the exterior plate.

In conclusion, we have discussed some general aspects of flexural wave scattering in the context of Mindlin's theory. For example, the identity (17) gives the conservation of energy flux for time harmonic waves in terms of the basic potentials. Although the flux identity (17) appears to be quite different in form from the flux identity (18) in Kirchhoff theory, in the limit of frequency approaching zero the two identities are equivalent. The optical theorem in Mindlin plate theory is identical to that of Kirchhoff plate theory and of two-dimensional acoustics because in the far-field the flexural waves are governed by a Helmholtz equation. The general formulation for scattering from circular inclusions is relatively straightforward using the potentials W_1 , W_2 and V for the displacement variables.

Acknowledgements

The work of A.N. Norris was supported by the US Office of Naval Research, and that of C. Vemula by Exxon Research and Engineering Co.

Appendix A. Wave solutions of Mindlin's equations

In the Kirchhoff plate theory the rotation is not an independent variable but is specified by the deflection according to $\psi = -\nabla w$. We therefore consider solutions of the form

$$\psi = A\nabla w,\tag{A.1}$$

where A is a constant. Using Eq. (A.1), the Mindlin equations (4a) and (4b) with zero applied load (q = 0) reduce to

$$DA\nabla^2 w - \overline{\mu}(A+1)w = A\frac{mh^2}{12}\frac{\partial^2 w}{\partial t^2}, \qquad \overline{\mu}(A+1)\nabla^2 w = m\frac{\partial^2 w}{\partial t^2}.$$
 (A.2)

Rearrangement of Eqs. (A.2) gives

$$\nabla^2 w + k^2 w = 0, (A.3a)$$

$$\frac{\partial^2 w}{\partial t^2} + \frac{\overline{\mu}}{m} k^2 (A+1) w = 0, \tag{A.3b}$$

where

$$k^2 = \left(\frac{h^2}{12}A - \frac{D}{\overline{\mu}}\frac{A}{(A+1)}\right)^{-1}.$$
 (A.4)

The only possible solution of Eq. (A.3b) *must* be time harmonic, forcing us to consider motion of the form $w(\mathbf{x}, t) = \text{Re}[W(\mathbf{x})e^{-i\omega t}]$, in which case Eq. (A.3b) implies

$$\frac{\overline{\mu}}{m}(A+1)k^2 = \omega^2. \tag{A.5}$$

Eqs. (A.4) and (A.5) are consistent if and only if $k = k_j$ and $A = A_j$, j = 1 or 2, as defined in Eqs. (7) and (9). A different kind of solution can be obtained by assuming w = 0, so that Eqs. (4a) and (4b) simplify to

$$\frac{1}{2}D(1-\nu)\nabla^2\psi - \overline{\mu}\psi = \frac{mh^2}{12}\frac{\partial^2\psi}{\partial t^2}, \quad \nabla \cdot \psi = 0. \tag{A.6}$$

The latter equation is satisfied by $\psi(\mathbf{x}, t) = -\mathbf{e}_z \times \nabla \phi(\mathbf{x}, t)$, where the scalar potential ϕ satisfies a modified wave equation,

$$\frac{1}{2}D(1-\nu)\nabla^2\phi - \overline{\mu}\phi = \frac{mh^2}{12}\frac{\partial^2\phi}{\partial t^2}.$$
(A.7)

This reduces to the Helmholtz equation (6c) for time harmonic motion $\phi(\mathbf{x}, t) = \text{Re}[V(\mathbf{x})e^{-i\omega t}]$.

We have shown that the displacement and rotation of Eq. (5) is a general solution for time harmonic motion. Conversely, it can be easily shown that any time harmonic motion must be of this form; that is, composed of a linear combination of the three solutions obtained here.

References

- [1] A.N. Norris and C. Vemula, "Scattering of flexural waves on thin plates", J. Sound Vib. 181, 115-125 (1995).
- [2] R.D. Mindlin, "Influence of rotary inertia and shear on flexural motion of isotropic, elastic plates", J. Appl. Mech. 18, 31-38 (1951).
- [3] R.D. Mindlin, "The thickness shear and flexural vibrations of crystal plates", J. Appl. Phys. 22, 316 (1951).
- [4] Y.-H. Pao and C.C. Chao, "Diffractions of flexural waves by a cavity in an elastic plate", J. AIAA 2, 2004-2010 (1964).
- [5] T.-H. Lu, "Diffraction of flexural waves by a circular rigid inclusion in an elastic plate and dynamic stress concentration", Master's Thesis, National Taiwan University, Taiwan (1966).
- [6] K.F. Graff, Wave Motion in Elastic Solids, Dover, New York (1991).
- [7] J.D. Achenbach, Wave Propagation in Elastic Solids, North-Holland, London (1973).
- [8] L.D. Landau and E.M. Lifshitz, Theory of Elasticity, 2nd Edition, Pergamon Press, Oxford (1964).
- [9] Y.I. Bobrovnitskii, "Calculation of the power flow in flexural waves on thin plates", J. Sound Vib. 194, 103-106 (1996).
- [10] A.W. Leissa, Vibration of Plates, Acoustical Society of America, Woodbury, New York (1993).
- [11] M. Born and E. Wolf, Principles of Optics, Macmillan, New York (1964).